THE PENNSYLVANIA STATE UNIVERSITY
SCHREYER HONORS COLLEGE

DEPARTMENT OF CHEMICAL ENGINEERING

MODELING THE EFFECT OF TEMOZOLOMIDE ON BRAIN TUMOR GROWTH

TAMARA LYNNE SISKIND

SPRING 2010

A thesis
submitted in partial fulfillment
of the requirements
for a baccalaureate degree
in Chemical Engineering
with honors in Chemical Engineering

Reviewed and approved* by the following:

Antonios Armaou
Associate Professor of Chemical Engineering
Thesis Supervisor

Ali Borhan
Professor of Chemical Engineering
Honors Adviser

*Signatures are on file in the Schreyer Honors College.

ABSTRACT

Glioblastoma multiforme is a type of brain tumor and is among the most difficult to treat cancers. Only two drugs have been approved by the FDA for treatment of glioblastoma multiforme: temozolomide and bevacizumab. Although these drugs have been approved for treatment, methods of treatment still need to be optimized. The objective of this thesis is to investigate a method of modeling the chemotherapeutic agent temozolomide in the Vital-Lopez computer simulation of a brain tumor. Research was done to develop a temozolomide component to be added to the Vital-Lopez model. Areas of investigation include representation of spatial distribution of temozolomide in brain tumors and simulation of apoptosis (programmed cell death) of tumor cells in response to different levels of temozolomide. The experimental literature on which the modeling was based is presented. The method and results of key parameter estimation are discussed. Finally, recommendations are made for further research.

TABLE OF CONTENTS

LIST OF FIGURES

ACKNOWLEDGEMENTS

The author would like to acknowledge Francisco G. Vital-Lopez for his patience, mentoring and direction, Dr. Antonios Armaou for his time and guidance as thesis supervisor, and Dr. Ali Borhan for his support as honors adviser.

Introduction

Brain cancer has received attention from the medical research community because it continues to be one of the most lethal and difficult to treat cancers. Researchers working on this field of research seek to combine their computational ability with developments in cancer biology to advance the understanding of how brain tumors progress. The ultimate goal of this research direction is to develop better treatments by using simulations to improve understanding of brain tumors. Improved computational models of tumors are of value because *in silico* experiments can help direct *in vitro* and *in vivo* experimentalists to select optimal conditions.

The classification of brain cancers is based on the different types of cells from which the tumor forms as well as the location in which the tumor begins to grow. Tumors that arise in the glial tissue of the brain are called glioblastomas. Though there are many other types of brain tumors, the scope of this paper is limited to a discussion of glioblastoma.

Existing Computational Model

Vital-Lopez *et al.* developed a 3-D model of a brain tumor responding to a host of biochemical cues [1]. To show how cancer cells migrate according to these biochemical cues, a process called *chemotaxis*, it is important to show the distributions of various chemical species in space and time. The distributions of nutrients are represented by PDEs that account for transport from the vasculature, diffusion, consumption and degradation. Nutrients are brought to the tissue by transport from the blood. The model includes a vascular network that behaves as a "source" term in the nutrient equations.

An agent-based model of the cells is used; the fate of each cell is determined by a stochastic process depending on local nutrient concentration gradients. The cells may divide, remain quiescent, undergo chemotaxis towards a region of higher nutrients, or become necrotic. The Vital-Lopez model simulates these cellular processes during uninhibited tumor progression. However, it does not currently simulate the action of a chemotherapeutic drug.

Honors Research Objective

The goal of this thesis research was to incorporate a chemotherapeutic drug in the Vital-Lopez agent-based brain tumor model. Modeling a chemotherapeutic drug allows for the simulation of treatments. To accomplish this goal, it was necessary to select a chemotherapeutic agent and research its mechanism of action, distribution, and toxicity.

Chapter 1: Temozolomide as a Therapeutic Agent

Current Therapies for Glioblastoma

Standard treatments for glioblastoma include surgery, radiation therapy, and radiation therapy combined with chemotherapy [2]. The scope of this paper was limited to studying the tumor response to a chemotherapeutic drug. In the United States, the FDA has only approved two chemotherapies for treatment of glioblastoma: bevacizumab and temozolomide.

Bevacizumab

In May 2009, the FDA approved bevacizumab, commercially named Avastin by Roche Pharmaceuticals. As shown in Figure 1, bevacizumab interferes with extracellular signaling pathways.

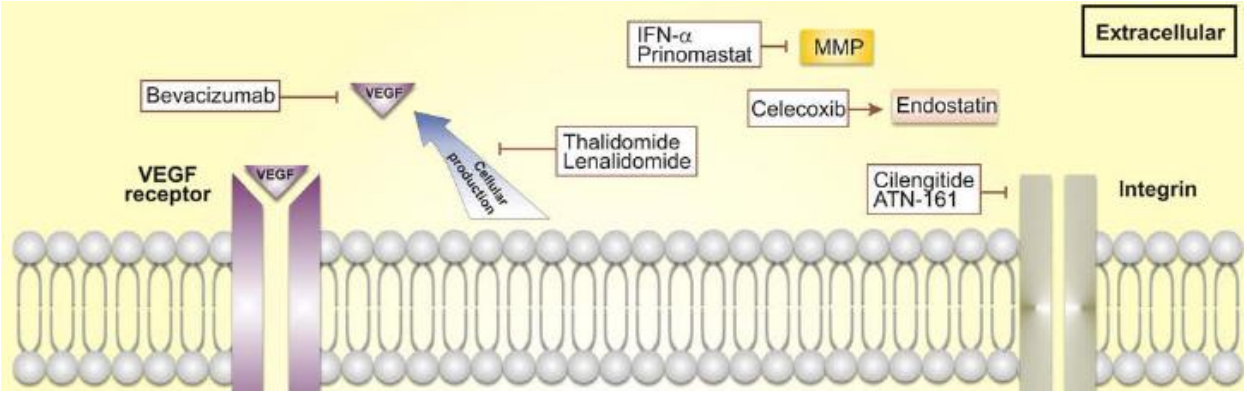

Figure 1: Angiogenesis Extracellular Signaling Molecules and their Inhibitors
Source: *M. L. Wong, A. Prawira, A. H. Kaye and C. M. Hovens. (2009, Sep). Tumour **angiogenesis**: Its mechanism and therapeutic implications in malignant gliomas. J. Clin. Neurosci. 16(9), pp. 1119-1130.*

Bevacizumab is a monoclonal antibody for VEGF, a type of growth factor secreted by cancer cells. VEGF recruits endothelial cells that migrate up the VEGF concentration gradient to form new capillaries. By deactivating the growth factor, bevacizumab prevents the tumor from recruiting new blood vessels, a process known as angiogenesis.

Temozolomide

Temozolomide was approved by the FDA for treatment of glioblastoma multiforme in 2005. In contrast to bevacizumab, temozolomide is a chemotherapeutic drug that acts on biochemical pathways that occur intracellularly. The mechanism is summarized in Figure 2. Temozolomide spontaneously converts to 5-(3-methyltriazen-1-yl) imidazole-4-carboximide (MTIC). MTIC undergoes conversion to an alkylating cation that transfers a methyl group to DNA [5]. While DNA is methylating in several places, the most critical methylation site is the O^6 position of guanine. The methylation of guanine at this site is

believed to cause double strand DNA breaks upon replication. These double strand breaks cause cell death (apoptosis) after the repeated cell divisions characteristic of tumors.

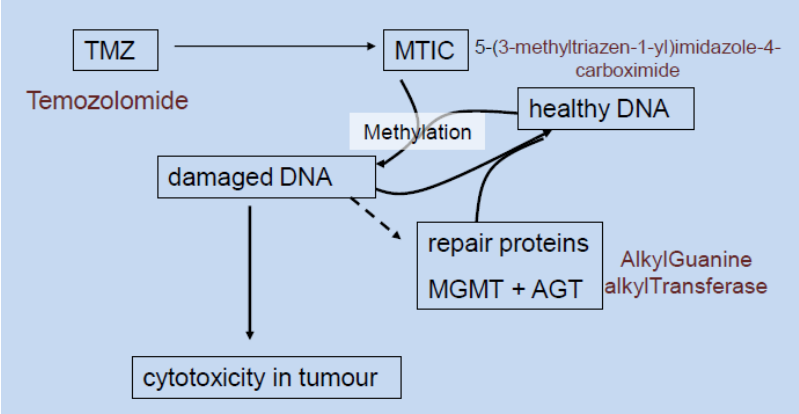

Figure 2: Overall Mechanism of Temozolomide Pathway

Cells have a natural repair-mechanism for fixing double-strand breaks. Proteins known as alkyl transferases can remove methyl groups from DNA, thereby counteracting the cytotoxic effect of the methylation [5]. Alkyl transferases are consumed in the process of demethylating DNA; it is possible for these repair proteins to become depleted. In rapidly dividng cells that have been methylated, the alkyl transferases can not be replenished quickly enough to fix the damage. Temozolomide resistance occurs when tumor cells express high levels of AGT proteins. However, inhibiting AGT proteins as well as alternate dosing schedules are under consideration for overcoming this type of resistance [5].

Selection of Temozolomide for Modeling

Temozolomide was selected for further study in this project. Varying the doses of temozolomide, a practice called metronomic dosing, has gained interest as a possible method to overcome tumor resistance to temozolomide. Although bevacizumab is anti-angiogenic but not cytotoxic, there is evidence that metronomic dosing of temozolomide can be anti-angiogenic in addition to cytotoxic [4]. Another reason for studying metronomic dosing of temozolomide is the mounting evidence that metronomic dosing might counteract certain types of tumor resistance to the drug [5].

In this study, the focus was on studying only temozolomide dosing because modeling the effect of bevacizumab requires a detailed description of tumor-induced vasculature remodeling, which has not been yet developed in the current model. Because of this, modeling bevacizumab's therapeutic mechanism was much more difficult with the current model as compared to modeling the cytotoxicity of temozolomide.

Previous Modeling

Compartmentalized models of temozolomide brain tissue concentration as a function of blood plasma concentration have been developed [6, 7]. A compartmentalized model assumes uniform concentration in each compartment. These models provide *overall* concentration, but do not describe the spatial distribution of temozolomide within the brain tissue. One goal of this project is to estimate parameters that allow for modeling how drug concentration varies in space.

A review of modeling the action of temozolomide in a tumor shows a range of approaches. Powathil *et al* model radiation followed by treatment of temozolomide [8]. The temozolomide portion of the Powathil model assumes that the cells killed by temozolomide is proportional to the tumor cell population. Stamatakos *et al* have developed a spatiotemporal tumor model based on individual patient's imaging, histopathologic, and genetic data [9]. The models reviewed do not consider the spatial gradients of temozolomide in the brain tumor.

Chapter 2: Modeling the Spatial Distribution of Temozolomide

The goal of this portion of the project was to obtain the parameters that determine the distribution of temozolomide. The parameters considered were diffusivity (D), degradation rate (k_D), and the mass transfer coefficient for temozolomide transport between blood plasma and brain tissue (K_T). After estimating D and k_D from various literature data, mass transfer equations and a steady-state assumption were used to fit a value of K_T.This parameter was fit to match experimental blood plasma and brain tissue overall concentration data from the literature. A simplified 2-D geometry and vasculature were used to estimate a K_T parameter for temozolomide, which provided an initial guess to be used in the 3D model.

Experimental Data on Temozolomide Distribution

Experimental data for overall brain tissue concentration as a function of plasma concentration has been collected and fit to models [6], [7]. Although data on the concentration of temozolomide in brain tissue is preferred, often experimentalists were better able to measure concentration of temozolomide in cerebrospinal fluid (CSF). In one study by Zhou *et al*, concentrations of temozolomide in both the brain tissue (C_{brain}) and CSF (C_{CSF}) were tracked over time [7].

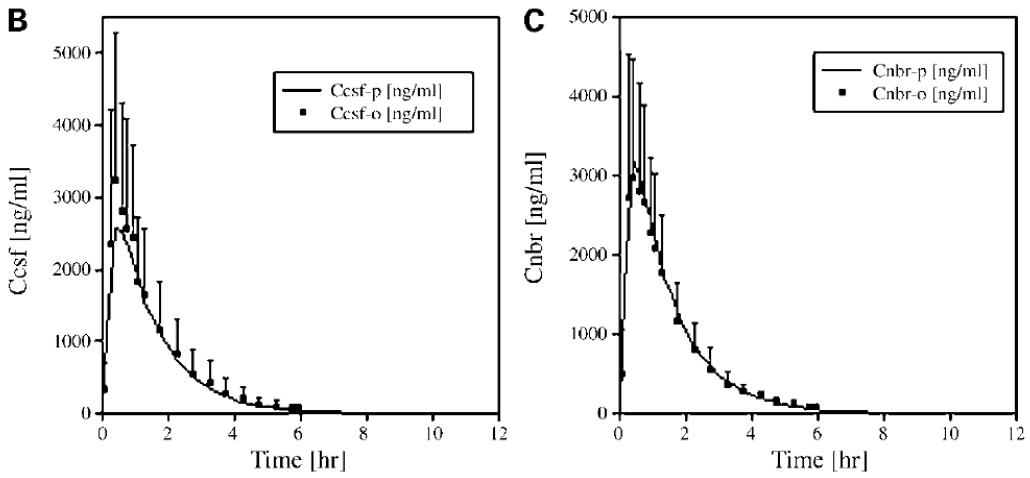

Figure 3: Concentration-Time Plots of Temozolomide in Cerebrospinal Fluid (CSF) and Brain Tissue (nbr)
Source: Q. Zhou, P. Guo, G. D. Kruh, P. Vicini, X. Wang and J. M. Gallo. (2007, Jul 15). Predicting human tumor drug concentrations from a preclinical pharmacokinetic model of temozolomide brain disposition. *Clin. Cancer Res. 13(14)*, pp. 4271-4279.

This experiment verifies that the concentration-times profiles of temozolomide in the CSF are a similar in magnitude and time scale. More detailed information was available for temozolomide concentrations in the CSF, which for the purposes of this chapter were assumed to be close to brain tissue concentrations.

$$C_{brain} \approx C_{CSF}$$

Approximating C_{brain} by C_{CSF} allows the use of mathematical models for concentration-time profiles of temozolomide concentrations in the blood plasma (C_p) and CSF (developed by Ostermann *et al*[6]). The Ostermann model describes the C_{CSF} and C_p as a function of temozolomide dose and time based on the set of differential equations (inset in Figure 4). The dose of temozolomide modeled in Figure 4 was 200 mg/m^2 at a body surface area (BSA) of 1.8 m^2. A_1 represents temozolomide in the gastrointestinal tract, A_2 represents temozolomide in the blood plasma, and A_3 represents temozolomide in the CSF. The CSF concentration given by Ostermann was used as an approximation of overall brain tissue concentration.

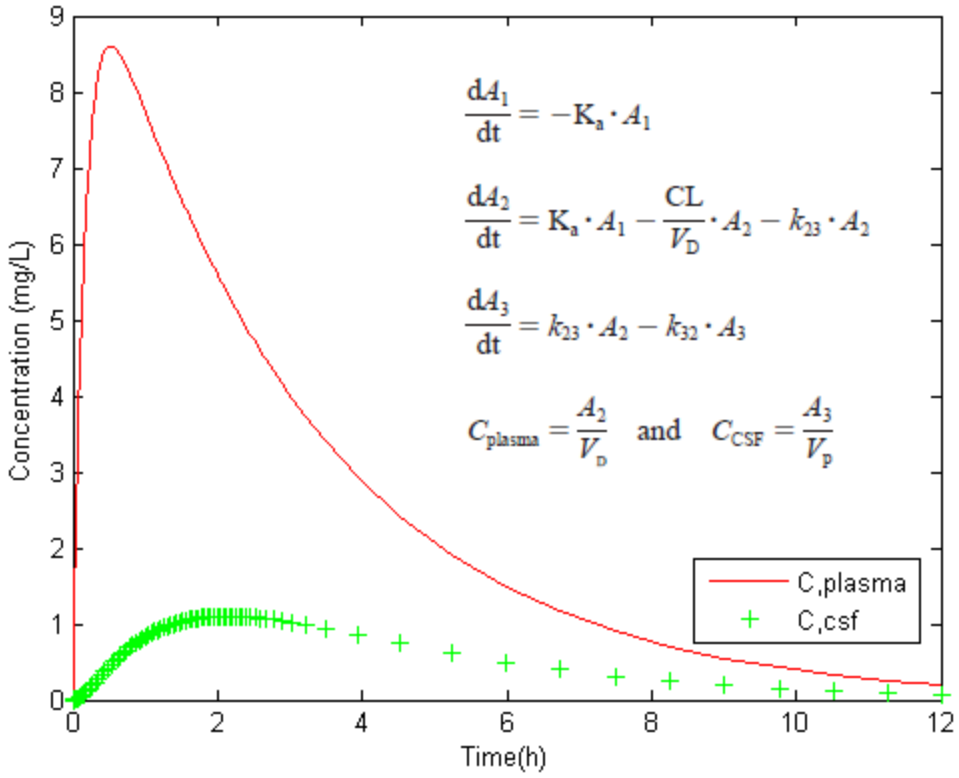

Figure 4: Plasma (red line) and CSF (green +) concentration-time profiles using the Ostermann model
inset: Ostermann model differential equations

Although concentration-time profiles of temozolomide data are common, researchers often condense this data into a single parameter by integrating the concentration-time curve to obtain an area-under-the-curve (AUC) value. AUC is a useful parameter because it can be divided by the time interval over which it was taken to obtain a time-averaged concentration, C_{AUC}.

$$C_{AUC} = \frac{AUC}{\Delta t} \qquad \text{(E2-1)}$$

To incorporate the behavior of temozolomide treatment in this model, it would be useful to have a plasma and brain tissue time-averaged concentrations every 2.5 hours, since the Vital-Lopez tumor model uses this time step (which is approximately the time in which a tumor cell migrates 20 μm). The AUC-averaged concentrations were taken from the Ostermann model and summarized in Table 1.

Table 1: Time-averaged Blood Plasma and CSF Concentrations from Ostermann

Time (h)	$C_{P,ave}$ (mg/L)	$C_{CSF,\ ave}$ (mg/L)
0-2.5	6.6	0.8
2.5-5	3.2	0.9
5-7.5	1.4	0.4
7.5-10	0.6	0.2
10-12.5	0.3	0.09

The $C_{CSF,ave}$ values were used as experimental values for overall brain concentration.

Modeling of Other Chemical Species

The concentrations of oxygen and growth factor TGFα are described by solving the following PDEs (partial differential equations) in space and time.

$$\frac{\partial S}{\partial t} = \nabla(D_S(t,z)\nabla S) + K_T^S(S_V - S) - k_S\, S \qquad \text{(E2-2)}$$

These equations account for the diffusion of species through tissue, with D_S representing the diffusivity of the species. K_T^S is a mass transfer coefficient between the bloodstream and the tissue, and k_S is a consumption term of species S in the tissue. S_V is the concentration of species S in the bloodstream.

In this model, a steady state assumption is used to solve for the spatial distribution of the species concentration. The PDEs are discretized using finite difference approximation. MATLAB (The MathWorks, Inc. Natick, MA.)is then used to solve a finite difference approximation of E2-3.

$$D_S\nabla^2 S + K_T^S(S_V - S) - k_S\, f(S) = 0 \qquad \text{(E2-3)}$$

Steady-State Assumption Remarks

Although the concentration of temozolomide is clearly changing with time, the steady-state assumption is used for several reasons. We use the steady-state assumption because the time-dependent problem requires the solution of a large-scale ODE (ordinary differential equation) problem, which is intractable with the current computational resources available. By re-solving the steady-state problem at each time step based on a new C_{plasma}, the "steady state" concentration in the tissue still changes at each time step. The concentration that is solved for is a function of only the present blood plasma concentration; the calculation does not require information from previous time steps. The steady state assumption, however, means that once C_{plasma} becomes negligible, so does C_{brain}. For the purposes of

estimating a mass transfer coefficient between the blood stream and brain tissue, the steady state assumption provides a useful starting point.

Diffusivity and Consumption Terms for Temozolomide

In the absence of literature values for temozolomide diffusivity, diffusivity of sodium caprylate, which has a similar molecular weight (MW_{SC} = 166.2; MW_{TMZ} = 194.2), was used. Geankoplis [10] reports the diffusivity of sodium caprylate in a BSA protein solution. The resistance to diffusion due to various biological solutes in brain tissue made selection of a protein solution more appropriate than a diffusivity value in water.

A consumption term was approximated using the half-life of temozolomide

$$k_{Degradation} \approx \frac{\ln(2)}{t_{1/2}}$$

The value of $t_{1/2}$ used was a 1-hour, the half-life value for brain tissue as reported in Zhou [7].

Mass Transfer Parameter Estimation for Temozolomide

For given values of D and k_d, an optimization problem was solved to minimize the sum of the deviation of the predicted average concentrations from the experimentally observed values by manipulating K_T.

First, a simplified 2-D geometry was used to obtain an initial guess. The characteristics of the simulation are summarized in Table 2.

Table 2: Characteristics of 2-D Simulation Domain

Discretization	20 μM
2-D Matrix Dimensions	11x11
Diffusivity	$7x10^{-10}$ m^2/s
Consumption	0.69 hr^{-1}
Boundary Conditions	No Flux

A simplified vasculature was considered: one straight vertical capillary and one straight horizontal capillary that are represented as “source” points. Points in the simulation domain without a capillary present are assumed to have no transport from blood, and the K_T term in those locations was set to zero.

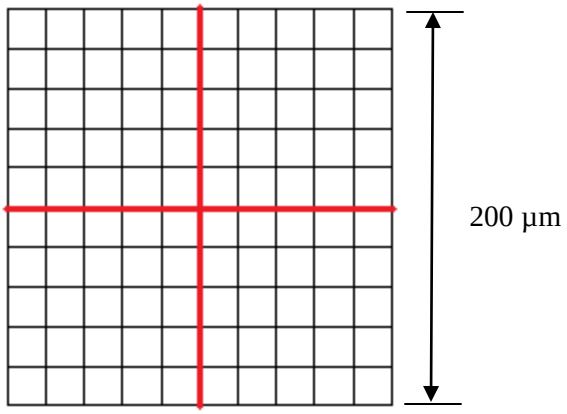

Figure 5: 2-D Simulation Domain with Simplified Vasculature

The vasculature considered in the 3-D simulation domain was more realistic. A depiction of this network is shown in Figure 6.

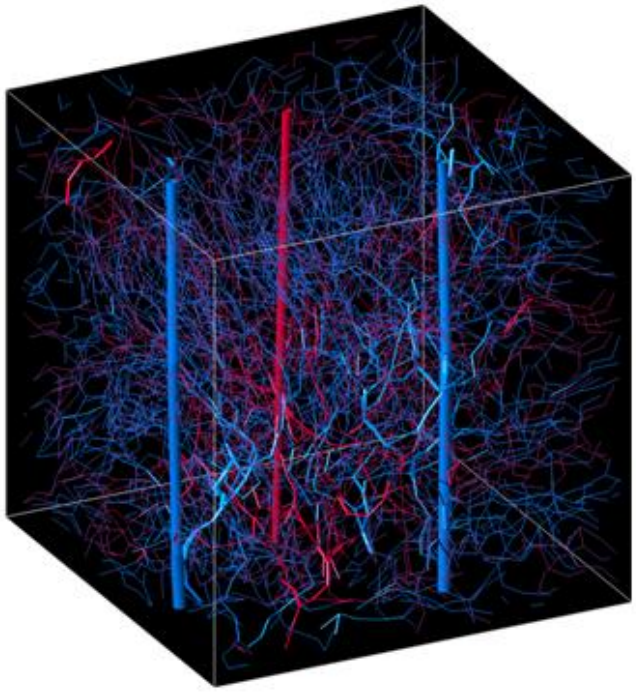

Figure 6: Vascular Network for 3-D Simulation

For each simulation domain, the finite difference approximation of E2-3 was solved. Overall concentration, $C_{ave,model}$, was computed from the average concentration of the simulation domain. An optimization of K_T was performed to match the overall model concentration with the expected time-averaged concentration from the Ostermann data. The data points from the Ostermann model used were those of Table 1. At each time point, the corresponding C_p value was used as the vasculature concentration "S_v" in E2. The concentration profile was determined by solving E2, and the average concentration, $C_{ave,model}$, was calculated.

The objective function of the optimization was the squared sum of the difference between $C_{ave,model}$, calculated from solving E2-3, and $C_{AUC,\,CSF}$, the average concentration computed from AUCs in the Ostermann model.

$$\textit{Objective function}: \min_{K_T} z = \sum_{i=1}^{5}\left(\frac{C_{AUC,CSF,i} - C_{AUC,CSF,model,i}}{C_{AUC,CSF,i}}\right)^2 \qquad \text{(E2-4)}$$

The MATLAB function "fminunc" was used to minimize the value of this objective function by varying K_T. A sensitivity analysis was performed by varying the values of D and k_T.

Results and Discussion

The value of K_T for this simplified geometry was found to be 1.83 hr^{-1}. The concentration-time profile with a 2.5-hour time step is shown in Figure 7.

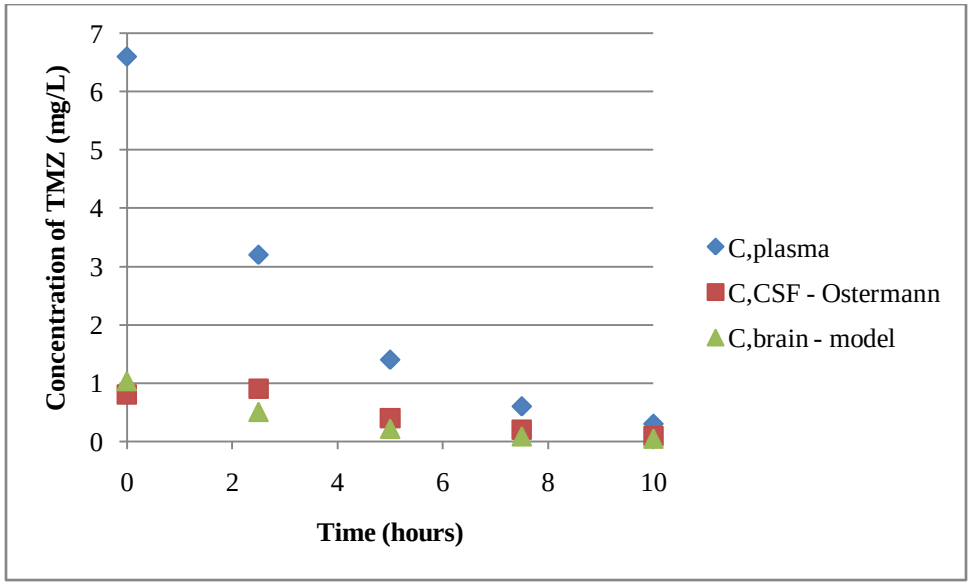

Figure 7: Model Steady-State Predictions of Brain Concentration

For the distribution and metabolism of temozolomide in the body, a time step of 2.5 hours is relatively coarse. The Ostermann models as well as the experimental data from Zhou show a concentration peak and subsequent drop-off in concentration that all occur during the first 2.5 hours after a dose of temozolomide is administered. Analysis of the time-averaged model also shows that the AUC is under-predicted. One alternative method of fitting K_T would be to match the AUC values instead of the concentrations. Another alternative would be to use a smaller time step. These possible venues will be pursued in future implementations of the research work.

By fitting a K_T value based on experimental data, we were able to represent a spatially-distributed concentration of temozolomide. Figure 8 shows the steady-state spatial distribution of the 2D model when the blood plasma temozolomide concentration is 6.6 mg/L.

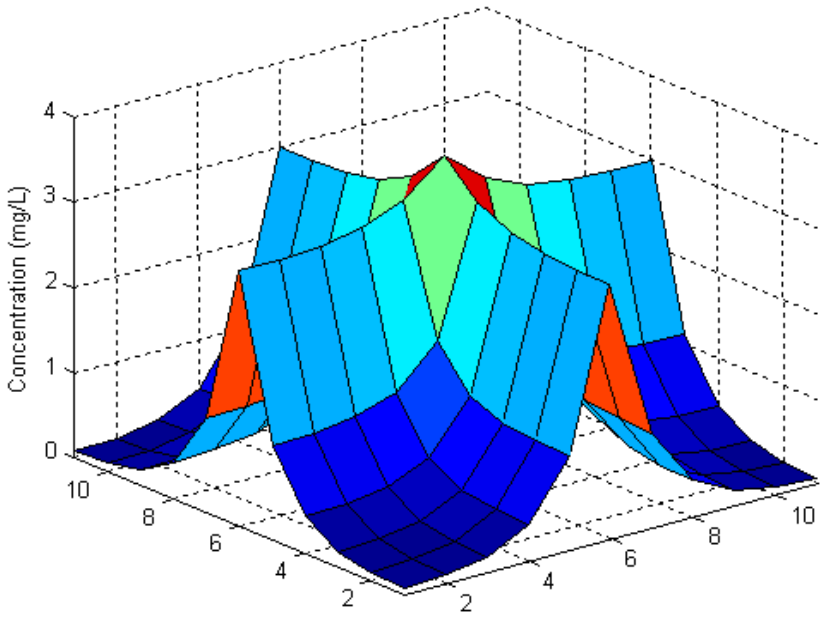

Figure 8: Pseudo-Steady State Temozolomide Distribution on 2-D Simulation Domain

A spatially-distributed concentration profile can account for differing levels of exposure to a drug based on proximity to a blood vessel.

Parameter Estimation in 3-D Simulation Domain

The D, k_d and K_T values obtained in the previous sections from the literature and the simplified model were used to estimate the K_T in the 3-D model. Although the 2-D model of Figure 5 is an oversimplification of the actual brain vasculature, it was useful for a first attempt at estimating parameters for computation of a spatially-distributed concentration profile. K_T for the 3D model was estimated in the same way as for the simplified model case by replacing the simplified model with the 3D model.

The optimized value of K_T for the 3D simulation domain was 1.10 hr^{-1}, which is lower than the simplified problem K_T of 1.83 hr^{-1}.

A sensitivity analysis of K_T to the value of $k_{degradation}$ and diffusivity is shown in Figure 9 for both the 3-D and 2-D simulations.

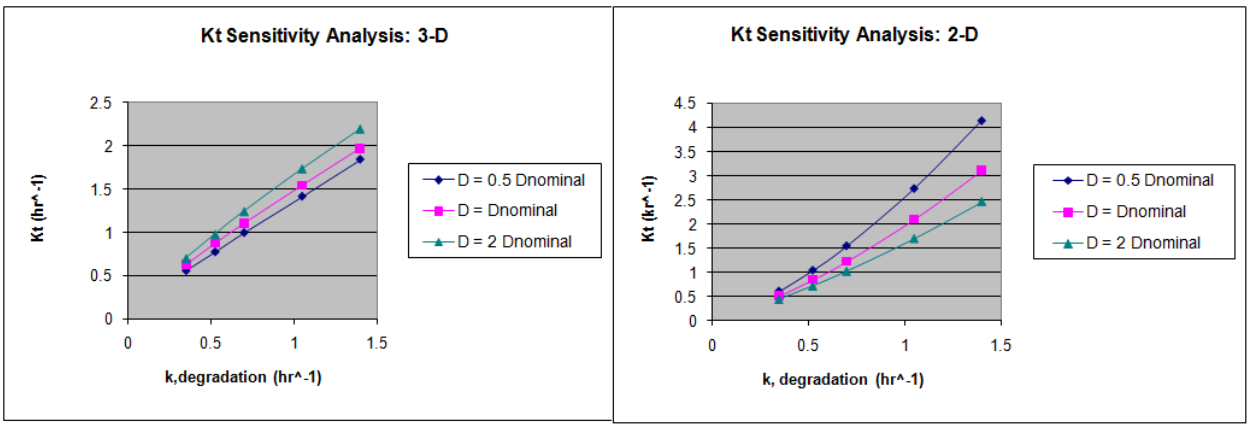

Figure 9: Sensitivity Analysis of Kt to k,degradation and diffusivity

The nominal diffusivity was the initial value from the previous section, $7x10^{-10}$ m^2/s and the nominal $k_{degradation}$ was 0.7 hr^{-1}. For both the 3-D and 2-D simulation domains, K_t is more sensitive to changes in the value of $k_{degradation}$ than changes in diffusivity. The 2-D problem was more sensitive to change than the 3-D problem. Although the 2-D problem was not expected to serve as a very realistic representation of the actual tumor space and vasculature, the range of 3-D K_t values fell within the range of 2-D problem K_t estimates.

The K_T value determined in the 3-D simulation was then applied to the 2-D problem. As expected for a similar K_T value, the resulting concentration-time profile was close to the initial 2-D problem profile.

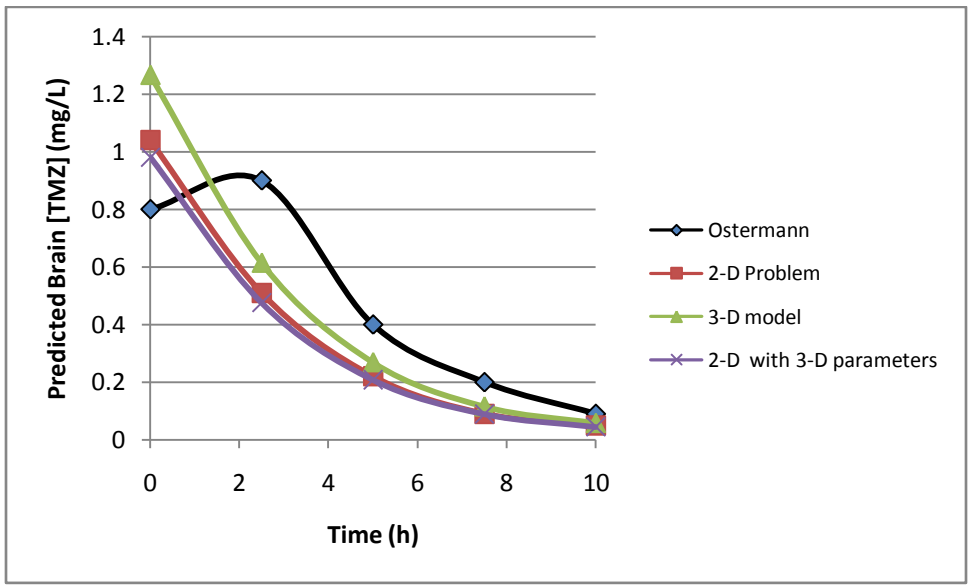

Figure 10: Applying 3-D Kt to 2-D Problem

Once again, the coarseness of a 2.5-hour time step results in an inability to predict the concentration peak at 2.5 hours.

Future Work

The pseudo-steady state assumption needs to be revisited. While this assumption may be reasonable for nutrients that are constantly circulating through the bloodstream, using this model means that the concentration drops to zero when temozolomide is no longer in the bloodstream. It is hypothesized that the important value may be area under the curve (AUC), and not specific concentration levels. How does AUC vary with space? Performing studies with smaller time steps could help elucidate the spatial distribution of AUCs.

Chapter 3: Modeling Toxicity of Temozolomide

Experimental Data on Temozolomide

Cytotoxicity studies of temozolomide report how much the growth of cells are inhibited at varying concentrations of drug. A commonly reported value is the IC-50 number, which is defined as the concentration at which the growth of cells is inhibited by 50%. This is quantified by comparing the total test population with the total control population at the end of the experiment.

Each cytotoxicity experiment can differ in number of initial cells studied, growth medium, duration of exposure to drug, and time points at which growth is measured. In one experiment by Baer *et al*, 750-1000 cells/well were grown on a plate and exposed to temozolomide for 5 days without media replacement [11]. The IC-50 value for human U-87 tumor cells in the Baer experiment was found to be 172 μM. In a different study by Kim *et al*, 1-3x10^3 cells/well were exposed to temozolomide with temozolomide-containing media replaced on a daily basis for 6 days [12]. The IC-50 value for human U-87 tumor cells in the Kim experiment was 9.87 μM. The lower value of IC-50 in the Kim paper can be explained by the daily replacement; the Baer experiment IC-50 value refers to the initial concentration, although as time passes and the media is not replaced, the final concentration of temozolomide is probably less than the reported value.

The Kim paper studied the inhibition of growth in three types of cells: rat brain tumor ("C6/LacZ" line), human brain tumor ("U-87MG" line), and human endothelial cells (bEnd.3). The effect of temozolomide on endothelial cells is of interest when considering temozolomide's anti-angiogenic effects.

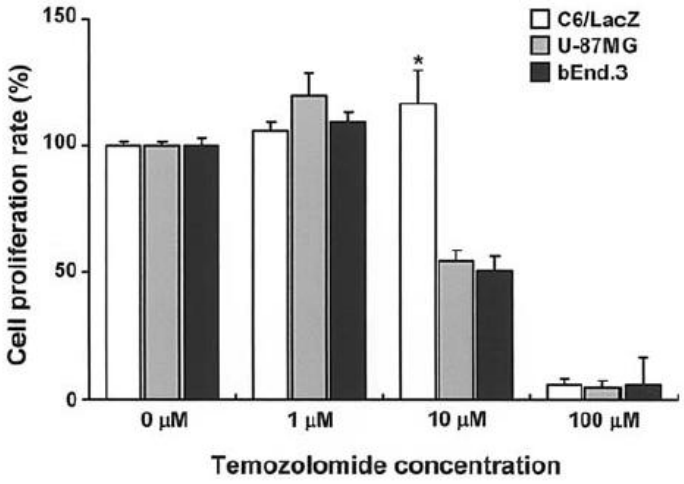

Figure 11: TMZ Inhibition of Growth of 3 Cell lines
Source: J. T. Kim, J. S. Kim, K. W. Ko, D. S. Kong, C. M. Kang, M. H. Kim, M. J. Son, H. S. Song, H. J. Shin, D. S. Lee, W. Eoh and D. H. Nam. (2006, Jul). Metronomic treatment of temozolomide inhibits tumor cell growth through reduction of angiogenesis and augmentation of apoptosis in orthotopic models of gliomas. Oncol. Rep. 16(1), pp. 33-39.

Although the Kim paper provides inhibition levels, it does not provide extensive information about growth kinetics. Most cytotoxicity papers only provide information about growth at the very beginning and very end of the experiement; to obtain information about growth kinetics of U87 cells, data from Tian *et al* was used to demonstrate non-inhibited growth kinetics [13].

Modeling Growth

From knowledge of the mechanism of temozolomide, it is evident that cells must be dividing to experience the progressive DNA damages that cause apoptosis. For this reason, it is helpful to distinguish between quiescent (non-dividing) and proliferating (dividing) cells in a model of growth. A quiescent cell (Q) can turn into a proliferating cell (P) at a rate of k_1, and a proliferating cell can divide into two daughter quiescent cells at a rate of k_2. Growth can then be modeled by the following equations, where total population, T, refers to the sum of all cells, regardless of type.

$$Q \xrightarrow{k_1} P \qquad P \xrightarrow{k_2} 2Q$$

$$dP/dt = k_1Q - k_2P \qquad \text{(E3-1)}$$

$$dQ/dt = 2k_2P - k_1Q \qquad \text{(E3-2)}$$

$$T = Q + P \qquad \text{(E3-3)}$$

If the ratio of proliferating to quiescent cells is assumed to be constant, E3-1 and E3-2 can be added together to form a first-order growth rate equation in terms of total population T:

$$dT/dt = k_2P = k_2\alpha T = k_T T \qquad \text{(E3-4)}$$

Here, α represents the fraction of total cells that are proliferating; (1- α) is the fraction of quiescent cells. An α value of 0.6 was used in our simulations; values of α reported in the literature range from 0.4 to 0.8 [14], [15]. Experimental data can then be used to fit k_T and thus k_2. Making the fixed-proliferating-fraction assumption to provide initial conditions of the quiescent and proliferating populations, it is then possible to fit k_1. Figure 12 shows the model-predicted proliferating, quiescent, and total population of cells as well as the experimental data for total population.

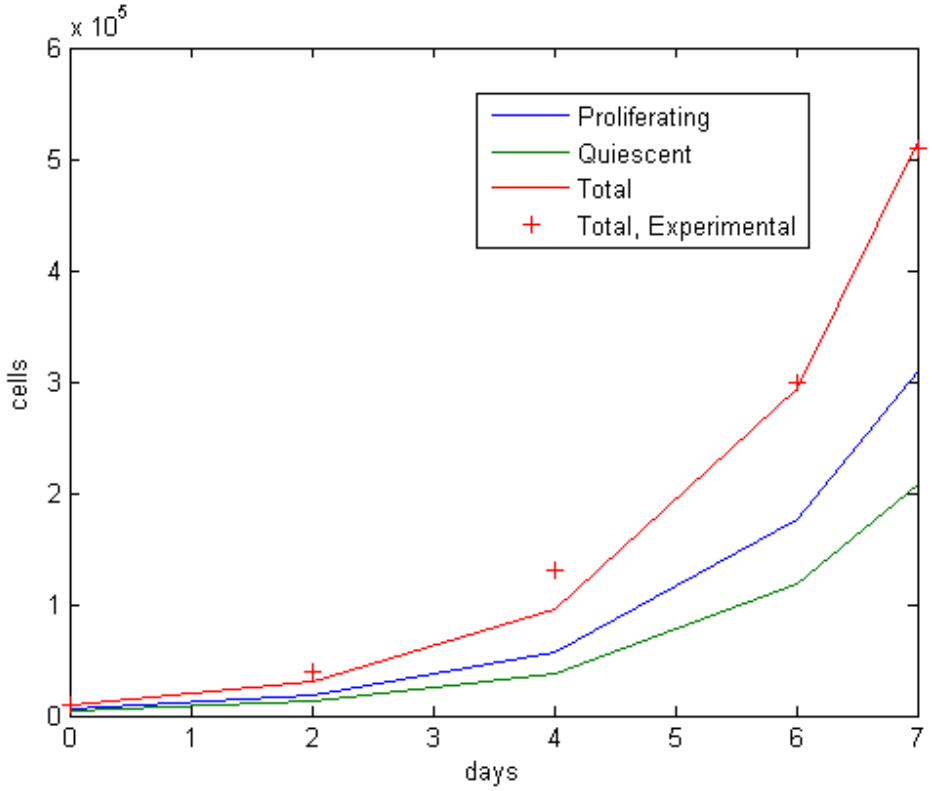

Figure 12: Fitting Tumor Growth (no TMZ inhibition)

The purpose of modeling normal tumor growth kinetics was to have a "base case" of uninhibited growth since the cytotoxicity experiments did not provide data such as final populations.

Modeling Inhibition Kinetics from Cytotoxicity of Temozolomide

The kinetics of growth inhibited by temozolomide include a term for apoptosis of proliferating cells; the differential equation for the population of proliferating cells changes has an additional term:

$$dP/dt = k_1Q - k_2P - \beta P \qquad \text{(E3-5)}$$

The parameter β represents the apoptosis of proliferating cells due to exposure to temozolomide. This parameter is a function of temozolomide concentration. The remaining population equations remain the same as in the previous section :

$$dQ/dt = 2k_2P - k_1Q \qquad \text{(E3-2)}$$
$$T = Q + P \qquad \text{(E3-3)}$$

It is assumed that the growth measurements only measure viable cells when reporting values of total cells T; the cells that undergo apoptosis are not accounted for in E3-3.

The fitted un-inhibited growth kinetic equations from the previous section were used to simulate a "base case" to determine the expected number of cells in the control group in the Kim cytotoxicity experiments. The k_1 and k_2 values determined for normal tumor growth were used and β values were determined by matching the population at day 6 to the experimental level as reported by Kim.

Experimental cytotoxicity data from Kim was used to fit β values at 10 and 100 μM levels of temozolomide. The Kim experiments were run for 6 days with an initial cell count of 10^3 cells/well. Based on the previous section model, the final population of cells in the control group, $N_{F,ctrl}$ would be $2.9*10^4$ cells/well. This value was taken to be the "100% growth" value. In the Kim experiments, the 1 μM sample did not show a noticeable reduction in growth. In fact, the sample grew slightly more than the control group.

TMZ Level (μM)	% proliferation rate
0	100
1	>100
10	50
100	5

Table 2: Experimental % Growth Inhibition
Source: J. T. Kim, J. S. Kim, K. W. Ko, D. S. Kong, C. M. Kang, M. H. Kim, M. J. Son, H. S. Song, H. J. Shin, D. S. Lee, W. Eoh and D. H. Nam. (2006, Jul). Metronomic treatment of temozolomide inhibits tumor cell growth through reduction of angiogenesis and augmentation of apoptosis in orthotopic models of gliomas. Oncol. Rep. 16(1), pp. 33-39.

With E3-2, E3-3, and E3-5 as governing equations, β values of 0.18 and 0.83 $days^{-1}$ were found for the 10 and 100 μM TMZ levels.

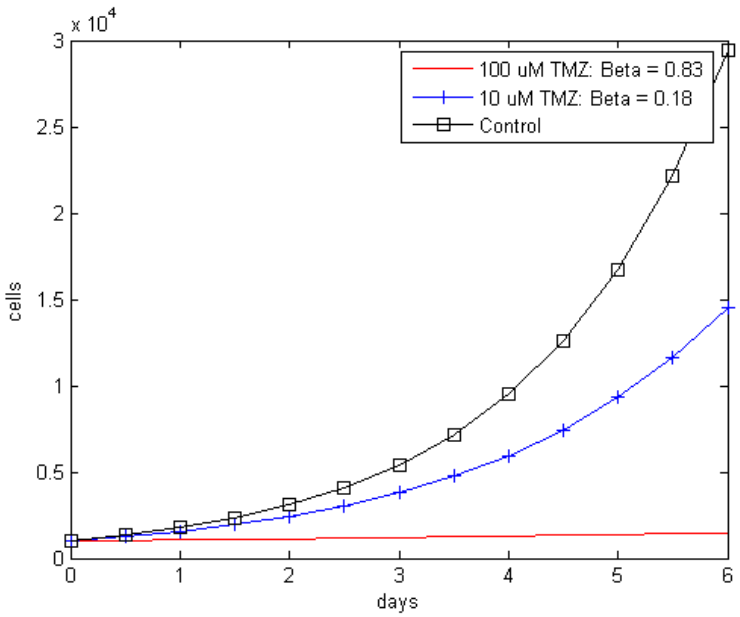

Figure 13: Population-Time Plots Using Inhibition Model

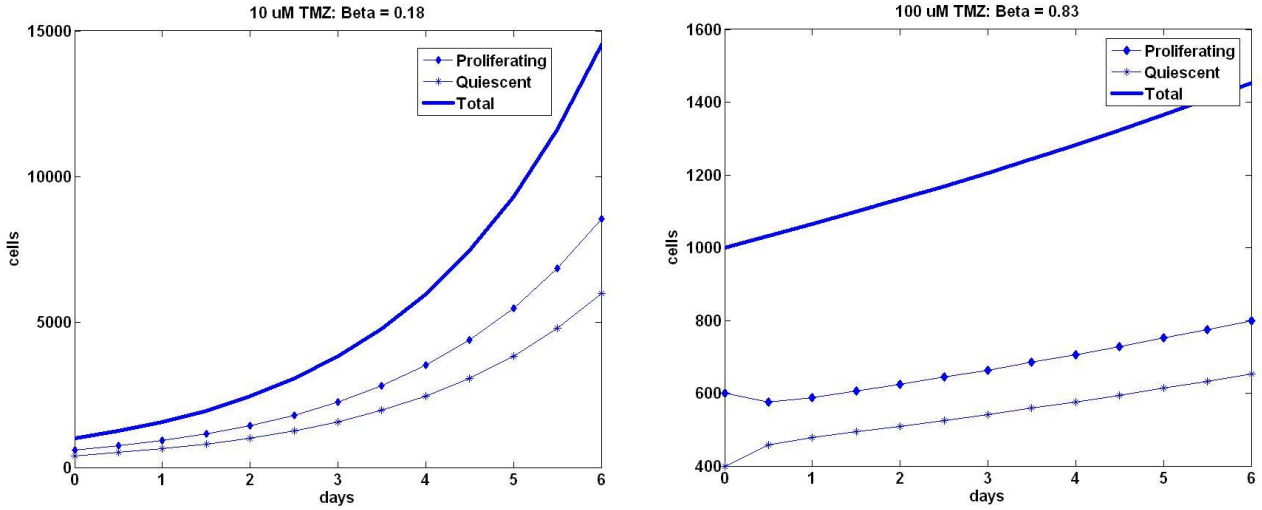

Figure 14: Quiescent/Proliferating Populations of 10 and 100 uM TMZ Inhibited Growth

Future Work

In this thesis, β parameters that represent apoptosis in a deterministic model were fit to match experimental cytotoxicity data. The next step towards integrating this information into a deterministic model is to convert the deterministic values into stochastic parameters that can be used with the Vital-Lopez model.

The population model represented by equations E3, E4, and E6 assumes only two types of cells; proliferating and quiescent. This model is assumed to be sufficient for the purposes of this project, which was to estimate the increased probability of apoptosis in dividing cells due to temozolomide exposure.

Bibliography

[1] F. G. Vital-Lopez, A. Armaou, M. Hutnik and C. D. Maranas, "Modeling the effect of chemotaxis in glioblastoma tumor progression," 2009.
[2] "FDA Approval for Bevacizumab - National Cancer Institute." *National Cancer Institute - Comprehensive Cancer Information.* N.p., n.d. Web. 27 Mar. 2010. <http://www.cancer.gov/cancertopics/druginfo/fda-bevacizumab>.
[3] "FDA Approval for Temozolomide - National Cancer Institute." *National Cancer Institute - Comprehensive Cancer Information.* N.p., n.d. Web. 31 Mar. 2010. <http://www.cancer.gov/cancertopics/druginfo/fda-temozolomide>.
[4] R. S. Kerbel and B. A. Kamen. (2004, Jun). The anti-angiogenic basis of metronomic chemotherapy. *Nat. Rev. Cancer. 4(6),* pp. 423-436.
[5] J. L. Villano, T. E. Seery and L. R. Bressler. (2009, Sep). Temozolomide in malignant gliomas: Current use and future targets. *Cancer Chemother. Pharmacol. 64(4),* pp. 647-655.
[6] S. Ostermann, C. Csajka, T. Buclin, S. Leyvraz, F. Lejeune, L. A. Decosterd and R. Stupp. (2004, Jun 1). Plasma and cerebrospinal fluid population pharmacokinetics of temozolomide in malignant glioma patients. *Clin. Cancer Res. 10(11),* pp. 3728-3736.
[7] Q. Zhou, P. Guo, G. D. Kruh, P. Vicini, X. Wang and J. M. Gallo. (2007, Jul 15). Predicting human tumor drug concentrations from a preclinical pharmacokinetic model of temozolomide brain disposition. *Clin. Cancer Res. 13(14),* pp. 4271-4279.
[8] G. Powathil, M. Kohandel, S. Sivaloganathan, A. Oza and M. Milosevic. (2007, Jun 7). Mathematical modeling of brain tumors: Effects of radiotherapy and chemotherapy. Phys. Med. Biol. 52(11), pp. 3291-3306.
[9] G. S. Stamatakos, V. P. Antipas and N. K. Uzunoglu. (2006, Aug). A spatiotemporal, patient individualized simulation model of solid tumor response to chemotherapy in vivo: The paradigm of glioblastoma multiforme treated by temozolomide. *IEEE Trans. Biomed. Eng. 53(8),* pp. 1467-1477.
[10] C.J. Geankoplis, E.A. Grulke and M.R. Okos. (1979 Apr). Diffusion and interaction of sodium caprylate in bovine serum-albumin solutions. *Industrial & Engineering Chemistry Fundamentals 18(3),* pp. 233-237.
[11] J. C. Baer, A. A. Freeman, E. S. Newlands, A. J. Watson, J. A. Rafferty and G. P. Margison. (1993, Jun). Depletion of O6-alkylguanine-DNA alkyltransferase correlates with potentiation of temozolomide and CCNU toxicity in human tumour cells. *Br. J. Cancer 67(6),* pp. 1299-1302.
[12] J. T. Kim, J. S. Kim, K. W. Ko, D. S. Kong, C. M. Kang, M. H. Kim, M. J. Son, H. S. Song, H. J. Shin, D. S. Lee, W. Eoh and D. H. Nam. (2006, Jul). Metronomic treatment of temozolomide inhibits tumor cell growth through reduction of angiogenesis and augmentation of apoptosis in orthotopic models of gliomas. Oncol. Rep. 16(1), pp. 33-39.
[13] X. X. Tian, Y. G. Zhang, J. Du, W. G. Fang, H. K. Ng and J. Zheng. (2006, Jun). Effects of cotransfection of antisense-EGFR and wild-type PTEN cDNA on human glioblastoma cells. Neuropathology 26(3), pp. 178-187.
[14] X. X. Tian, P. Y. Lam, J. Chen, J. C. Pang, S. S. To, E. Di-Tomaso and H. K. Ng. (1998, Oct). Antisense epidermal growth factor receptor RNA transfection in human malignant glioma cells leads to inhibition of proliferation and induction of differentiation. *Neuropathol. Appl. Neurobiol. 24(5),* pp. 389-396.
[15] H. C. Ugur, N. Ramakrishna, L. Bello, L. G. Menon, S. K. Kim, P. M. Black and R. S. Carroll. (2007, Jul). Continuous intracranial administration of suberoylanilide hydroxamic acid (SAHA) inhibits tumor growth in an orthotopic glioma model. *J. Neurooncol. 83(3),* pp. 267-275.

ACADEMIC VITA of TAMARA L. SISKIND

tls5035@psu.edu

Campus Address
266 Simmons Hall
University Park, PA 16802

Permanent Address
21 Franklin Drive
Smithtown, NY 11787

EDUCATION

Bachelor of Science Degree in Chemical Engineering
The Pennsylvania State University, University Park, PA, May 2010
Honors in Chemical Engineering
Honors Thesis Title: Modeling the Effect of Temozolomide on Brain Tumor Growth
Thesis Supervisor: Antonios Armaou

Academic Research and Work Experience
Chemical Engineering Teaching Intern
Algae Cell Culture Research
WISER Program Research in Fluid Dynamics

INTERNATIONAL EXPERIENCE

Global Engineering Education Exchange in Nancy, France
Ecole Européenne d'Ingénieurs en Génie des Matériaux

LEADERSHIP & COMMUNITY SERVICE

Study Group Facilitator
Community Outreach Volunteer
Women in Engineering Program, University Park, PA

Hurricane Relief Volunteer
Lagniappe Service Project, New Orleans, LA

WORK EXPERIENCE

Engineer (Intern), Sterile Processing Technology & Engineering
Merck Manufacturing Division, West Point, PA

Facilities Engineer (Intern)
Chevron N.A. Exploration and Production, Lost Hills, CA

COMPUTER & LANGUAGE SKILLS

Matlab	French (Verbal and Written Competency)	HYSYS
MS Office	PI ProcessBook	Minitab

AWARDS

The President's Freshman Award
The President Spark's Award
The Evan Pugh Scholar Award
Outstanding Facilitator Award – Women in Engineering Program